

Three-Dimensional CFD Analysis of the Hemodynamic Effect of Different Stent-to-Artery Deployment Ratios

A. Lotfi and T. J. Barber

Department of Mechanical and Manufacturing Engineering
The University of New South Wales, Sydney, NSW 2052, Australia

Abstract

In vascular cardiology, stenting coronary arteries with the diameter greater than that of the native artery has been used in an attempt to securely anchor the device against the arterial wall. Various stent-to-artery deployment ratios can be used by clinicians to implant the stent into the artery. However, stent expansion beyond the native artery diameter alters vascular hemodynamic scenarios. These alterations may cause endothelial denudation and promote neo-intimal hyperplasia. The optimal level of stent-to-artery diameter ratio to reduce the severity of vascular damage and consequently the risk of adverse clinical outcome has not yet been determined. This injury of the endothelium due to stent overexpansion has been shown to be influenced by hemodynamic factors such as local wall shear stress (WSS). The information on the gradient of blood flow velocity during stent deployment is therefore of clinical interest as it is proportional to the distribution of wall shear stress. While in vivo measurement of the fluid dynamics quantities including velocity profile, pressure and wall shear stress is challenging, computational fluid dynamics (CFD) can be a valid tool to analyse these vascular fluid dynamics quantities. In this study, a three-dimensional CFD analysis was used to examine the fluid flow in a patient-specific artery with particular emphasis on the effect of various stent-to-artery ratio diameters. The fluid was assumed to be incompressible, Newtonian and homogenous. Both the stent struts and the arterial wall were considered to be rigid and non-porous. The results of this study give insight into the understanding of the mechanisms that may contribute to vascular damage from stent-expansion.

Introduction

Stent placement has long been shown to be an effective technique for treatment of arterial stenosis which occurs due to atherosclerosis inside the artery. Although stents provide long-term luminal patency and prevent the artery from restenosis, incidence of in-stent restenosis and large absolute stent-induced damage, which associates closely with late neo-intimal thickening, remains the common clinical complication. Recent clinical trials have shown that the size of the stent [10], as well as the deployment stent-to-artery ratio [1, 13] can be an important contributor to the extent to which the artery is prone to in-stent restenosis. In addition, it has been revealed that these geometric differences caused by various stent sizes substantially influence vascular fluid dynamics quantities such as velocity profiles, pressure gradients and associated wall shear stress distribution. La Disa et al. [3] utilized computational fluid dynamics to study the WSS distribution and thus hemodynamic alterations through the canine coronary artery with respect to the stent-to-artery deployment ratios of 1.1 and 1.2. Their findings show that the stent expansion ratio of 1.1 is less likely to subject the arterial wall to low WSS, compared with stents inserted with a 1.2 stent-to-artery ratio. More recently, in 2013, Niu et al. [7] examined

the effect of degrees of oversizing deployments with a range of different stent-to-vessel ratios of 1, 1.125, and 1.25 on local hemodynamic and vascular biomechanics of vertebral artery ostial stenosis. They suggested that the deployment of stent with expansion ratio of 1.125 may be hemodynamically advantageous in order to minimize in-stent restenosis and hyperplasia.

Although the use of stent-to-artery expansion ratios of 1.1 to 1.25 have proven to be effective in reducing vascular damage during stenting arteries when offering a good luminal patency [12, 14], a higher stent-to-artery deployment ratios of 1.5, 1.75 and 2 might be required to better secure the stent against the arterial wall. However, no evidence of a correlation between this range of stent expansion ratio and the local hemodynamics such as velocity profile and arterial wall shear stress have been presented in the scientific literature yet. Hence, the aim of this work is to investigate different hemodynamic scenarios of stent oversize in the femoral artery using a computational fluid dynamics (CFD) model.

Methodology

Geometric Model

The geometry of the artery as well as deployed stent was created in SolidWorks (Dassault Systems) as shown in figure 1. The artery itself was modelled as a simple cylinder of length 520 mm divided into three sections: The upstream entrance section of length 120mm whose diameter is shrinking gradually from 5.9mm to 5mm, 4.4mm and 4mm towards the middle section, the middle section with diameter of 4mm, and the section beyond the middle segment which diameter is decreasing from 4mm to 3.7mm towards the downstream outlet. The stent was modelled with thickness and width of, respectively, 80 μ m and 170 μ m and the outer diameter of 4mm, which is equal to the native vessel diameter. This stent was then expanded with regards to five different degrees of stent-to-artery ratios of 1, 1.25, 1.5, 1.75 and 2 and placed at an angle of 0° to the middle section of the vessel. Five configurations of stented artery were tested with respect to above-mentioned different stent-to-vessel expansion ratios.

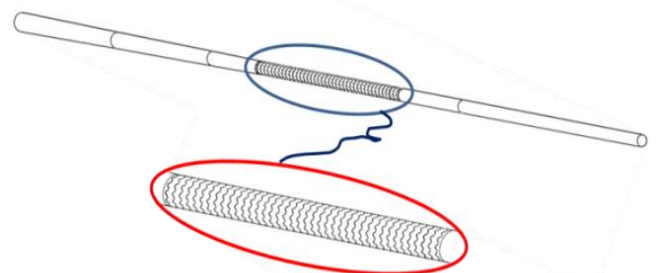


Figure 1. Schematic view of the stented femoral artery divided into three sections with stent placed at the middle section.

Numerical Model

The geometry was exported to ICEM 14.5 (ANSYS Inc., Canonsburg, PA, U.S.A) for grid discretization. A hybrid volume meshing technique developed by current authors [4] was applied due to its ability to capture the complex geometry of stented vessel. The ANSYS Fluent 14.5 (Fluent Inc., Lebanon, NH) package was then used to solve the Navier Stokes equations. The SIMPLEC algorithm was used for the pressure-velocity coupling for laminar steady-state fluid dynamic simulations. The momentum spatial discretization schemes were set to second order upwind. Blood was assumed to be incompressible, homogeneous and Newtonian with a viscosity and density of 0.0035 kg/ms and 1060 kg/m³, respectively. Newtonian flow in vessels of this size has been shown to be a reasonable assumption [5]. A mesh independence study was performed using different meshes (coarse, medium and fine) through wall shear stress along a line in the axial direction of the arterial wall with stent-to-vessel expansion ratio of 1. A constant paraboloid- shape velocity profile with mean velocity of 0.25 m/s was used for inlet velocity condition when the zero static pressure was set at the downstream outlet to unconstraint the inlet condition. The mean velocity value used in the present study was obtained from the pulsatile waveform regenerated from 100 time points. Each steady state simulation was performed on a computer that allowed for simulation convergence after 96 h. Fifteen simulations were taken into account to investigate spatial mesh dependence. Residual reduction to 10⁻⁶ of the primary value was set as a convergence criterion. The results were considered spatially independent of the computational mesh when the grid convergence index of a fine mesh varied by < 2% for WSS compared to a grid with higher cell density. As transient simulations required additional validation which was beyond the computational resources available for the present investigation, all simulations were performed under steady state condition neglecting the effect of oscillating flow. The vessel walls are assumed non-slip and rigid [2], and the movement of the artery was not implemented.

Wall Shear Stress Index

WSS as one of the indicators of disturbed flow is an important factor in the pathobiology of neo-intimal hyperplasia and in-stent restenosis [8]. In view of these considerations we tested the theory that different degrees of stent oversize influence indexes of WSS over adjacent intravascular cells. The threshold for comparing the distribution of low WSS was defined at 0.5 Pa as the luminal surface exposed to slightly below this value is shown to potentially contribute to the development of neo-intimal hyperplasia [9]. Moderate and high WSS threshold values which are unlikely contribute to intimal thickening are set to 0.5-2.5 Pa, and 2.5-12 Pa, respectively [9]. Higher values of WSS, particularly WSS>12 Pa are also considered in this study because the flow factors involved in platelet activation and thrombosis notably comprise this range of WSS and recirculation zones caused by stent deployment [6].

Results and Discussion

The influence of stent oversizing on the distribution of WSS in one of the femoral arteries is shown in figure 2. A large region of low WSS (<0.5 Pa) is clearly visible in all models. The extent of the low WSS area is highly dependent on the stent-to-artery expansion ratio. Regions of elevated WSS were localized at the surface of individual stent strut (for each simulation) and at the distal stent-artery transition for all stent expansion ratios excluding the first case. In contrast, low WSS surrounded the individual stent struts independent of the stent-to-artery diameter ratio. Regions of low WSS are evident in this figure, moving further downstream from the proximal stented area in the artery

with the deployment ratio of 1.25 towards the distal stented area when increasing the stent expansion ratio from 1.25 to 2.

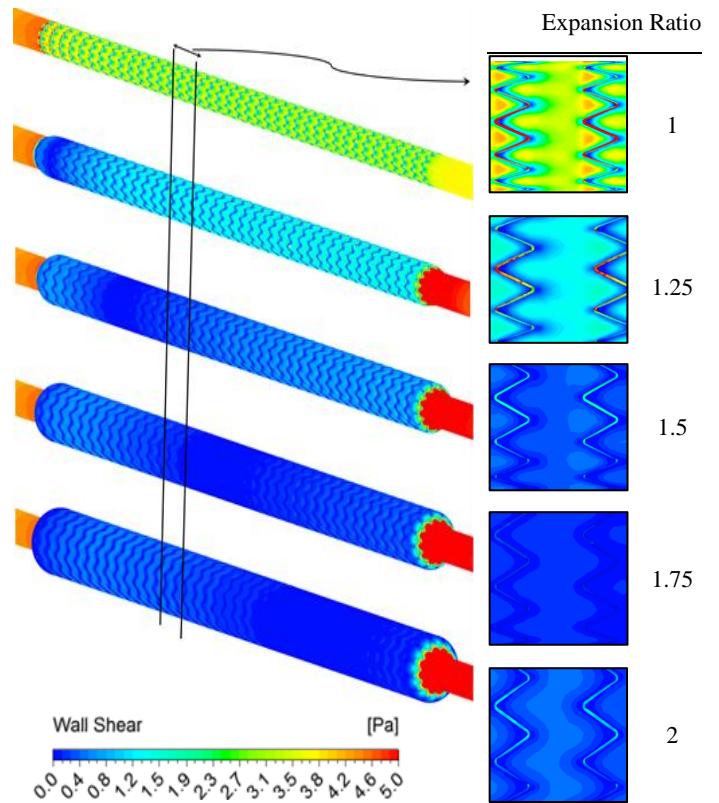


Figure 2. Wall shear stress distribution within the stented portion of five arteries with different sizes of stent-to-artery deployment ratios. The blood flow direction is from left to right.

The effect of different stent expansion diameter ratio on the local distribution of WSS within the stented portion of the artery is quantified in figure 3. As can be seen, a larger area of stented artery was exposed to low WSS when the diameter of the stent increased to the greater expansion ratios. It also shows that the higher WSS magnitudes found at the surface of individual stent strut dropped markedly with further increase of the stent-to-artery ratio within the stented vessel, excluding the WSS values localized at the distal stent-artery transition area which is obviously increasing with further stent ratio growth from 1 to 2.

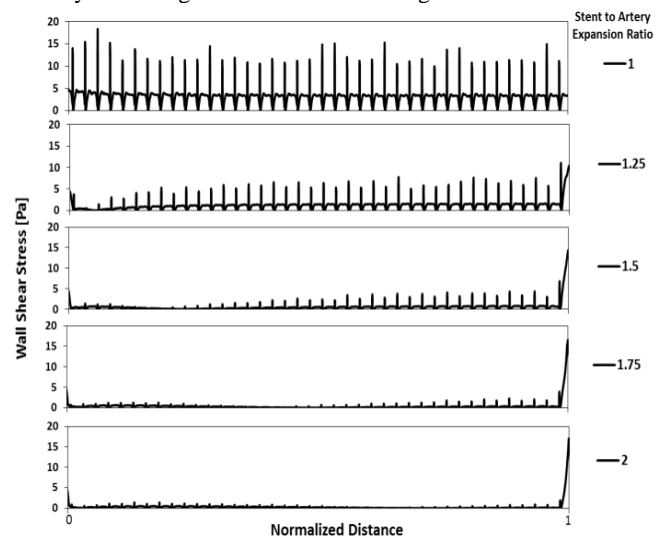


Figure 3. Comparison of the distribution of the wall shear stress on a line in the axial direction of the artery within the stented region for all five stent-to-artery deployment ratios

To understand why larger vascular wall areas are exposed to low WSS in the oversized stent segments local hemodynamics must be considered. The velocity pattern within the stented region of the vessel is illustrated in figure 4 for each simulation.

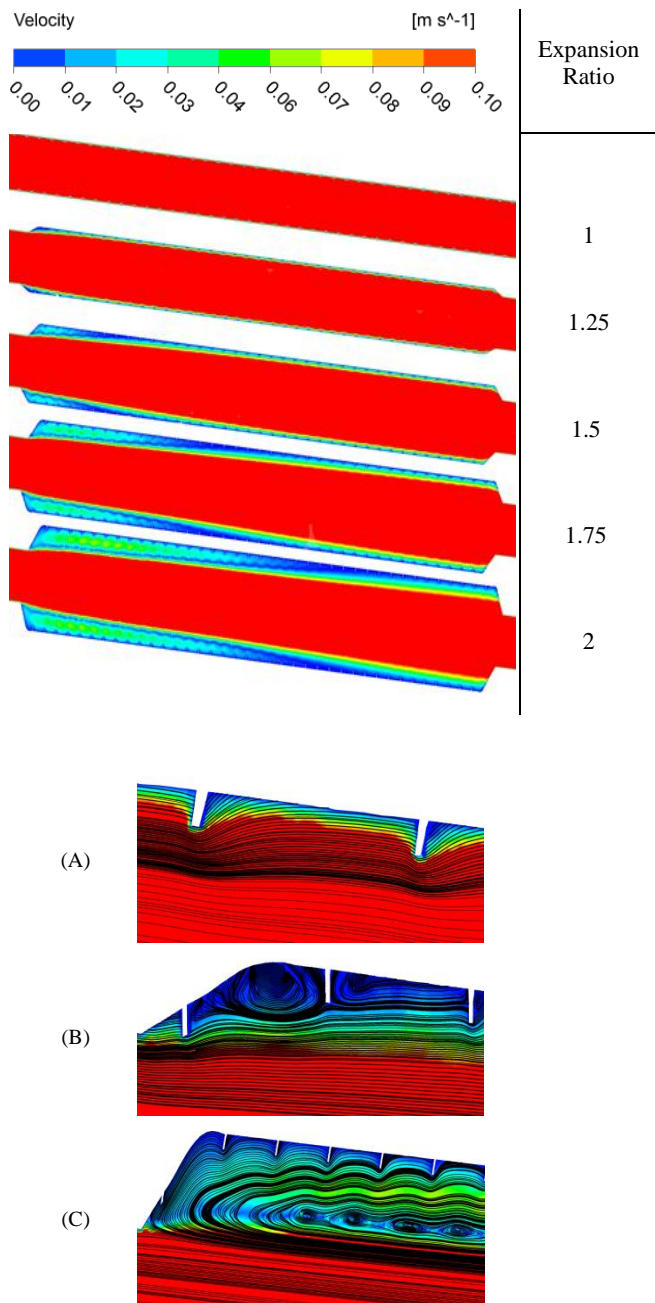


Figure 4. Velocity contour plots projected on the mid-longitudinal plane for five different configurations of the stented artery made with regard to various stent-to-artery expansion ratios.

Close up views: Projection of streamlines to middle cut plane in the vicinity of stent struts. (A) Streamlines over the second and third struts of the first case with no oversized stent deployment; (B) Recirculation zones adjacent to the stent struts of the model with stent expansion ration of 1.25; (C) Large area of recirculation in the oversized region of the last case with stent expansion ratio of 2.

As recognizable in figures 4 and 4A in the zoomed in view, smaller region of low near-wall velocities are found in the vicinity of stent struts for the first case at where regions of low WSS were localized compared to other cases.

With increasing the stent diameter ratio to 1.25 some breakups were found at the proximal oversized stented portion of the vessel near the stent strut, introducing recirculation zones adjacent to the stent struts (Figure 4B). Such near wall recirculation zones inherently yield low WSS values. The relative stent-to-artery expansion ratio alters the extent and level of this recirculating area and influences the location of the near-wall stagnation point along the artery. A large recirculation zone in the oversized segment of the artery is shown in figure 4C for clarification.

A further increase in the stent expansion ratio causes these vortices to be gradually dissipated through the overexpanded portion of the stented vessel as the velocity has slowed, resulting region of lower near-wall velocity adjacent to the luminal surface (see figure 4 for the expansion ratios of 1.5 to 2).

However, due to the higher velocity in the oversized segment of the stented artery with larger expansion ratio compared to that found for smaller ratios, the breakups die down farther downstream of the stented region, and the stented wall experiences a larger area of low near-wall velocity.

These findings confirm that an increase in stent expansion ratio exposes more of the luminal surface to distributions of low WSS as the vortices in the recirculating area are contracting down towards the arterial surface and producing a larger area of lower near-wall velocity.

The combined effect of local flow alterations induced by stent struts and a range of different stent-to-artery expansion ratio on the whole arterial surface is quantified in figure 5. There the distribution of low, moderate, high and greater than 12 Pa WSS is illustrated as the relevant parameter responsible for the biological response of arteries to stent deployment.

The histogram shows that more than 50 percent of the vessel wall was subjected to moderate and high WSS values which are unlikely to contribute to the development of intimal thickening for the stent expansion ratios of 1 and 1.25. Further increase of the stent deployment ratio exposed less of the luminal surface to distribution of these two ranges of WSS values.

However, altering the stent deployment ratio from 1 to 2 substantially produces an increase in the exposure of the vascular wall to the low WSS. The present results indicate that the luminal surface of the artery with stent expansion ratio of 1 may be the least prone to in-stent restenosis, compared to other stent-to-vessel ratios.

On the other hand, the use of this expansion ratio may predispose this vessel to thrombo-embolic complications as almost 1 percent of its luminal wall is exposed to the $WSS > 12$ Pa accompanied by platelet deposition at locations of relative low WSS. It is known that the flow factors involve in thrombo-embolic events contain this range of WSS (> 12 Pa) and recirculation zones caused by stent implantation [11].

Our results highlight the occurrence of these conjoint areas of low WSS and $WSS > 12$ Pa. These concomitant regions are more pronounced at the individual stent struts of the first case especially over the proximal stented region, as well as at the outlet of the stented portion of the vessel for the other cases.

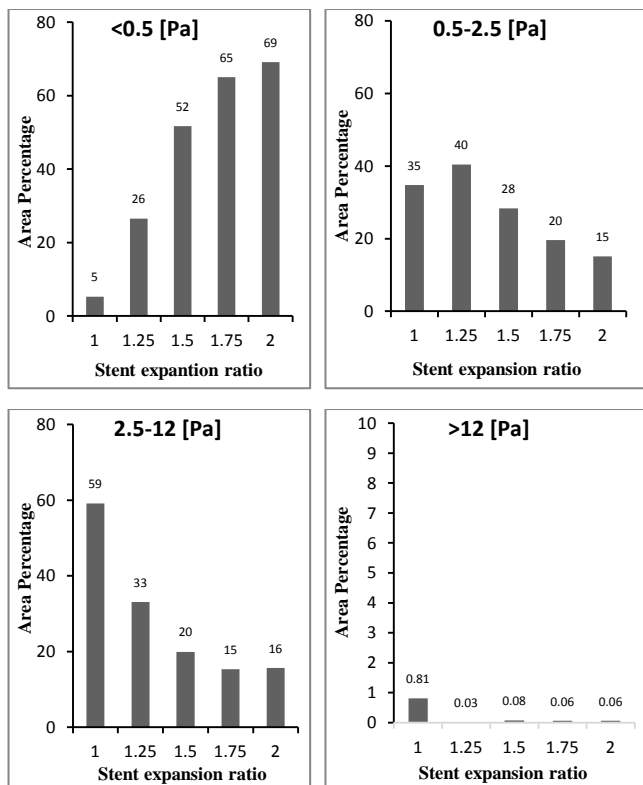


Figure 5. Percentage of the vessel wall area exposed to low (<0.5 Pa), moderate (between 0.5 and 2.5 Pa), high (between 2.5 and 12 Pa) and greater than 12 Pa (induces platelet aggregation) WSS for all five stent-to-artery expansion ratios.

Conclusions

This study shed light on the complex interplay between altered WSS pattern, and the development of plaque and thrombotic events, and the vulnerability process in the artery with different stent-to-artery ratios.

The results showed that the luminal surface that may be more susceptible to intimal thickening is markedly increasing with the growth of stent overexpansion ratio by adversely affecting the distribution of WSS.

The findings, however, indicated that the vascular damage produced by the stent overexpansion is not limited to the exposure of the arterial surface to the neo-intimal hyperplasia. The stent expansion beyond the luminal diameter may cause severe increases in WSS above 12 Pa that potentially may contribute to the platelets activation and expose the artery to the thrombo-embolic complications.

References

[1] Garasic, J.M., Edelman, E.R., Squire, J.C., Seifert, P., Williams, M.S., & Rogers, C., Stent and Artery Geometry Determine Intimal Thickening Independent of Arterial Injury, *Circulation*, **101**, 2000, 812–818.

[2] Ku, D.N., Blood Flow in Arteries, *Annu Rev Fluid Mech.*, **29**, 1997, 399–434.

[3] LaDisa, J.F. Jr., Olson, L.E., Guler, I., Hettrick, D.A., Audi, S.H., Kersten, J.R., Warltier, D.C., and Pagel, P.S., Stent Design Properties and Deployment Ratio Influence Indexes of Wall Shear Stress: A Three-dimensional Computational Fluid Dynamics Investigation Within a Normal Artery, *J Appl Physiol.*, **97**, 2004, 424–430.

[4] Lotfi, A. & Barber, T.J., Optimization of CFD Meshing for Stented Vessel Geometries, *Applied Mechanics and Materials*, **553**, 2014, 373–378.

[5] Marossy, A., Svorc, P., Kron, I., & Gresov, S., Hemorheology and Circulation, *Clin. Hemorheol. Microcirc.*, **42**, 2009, 239–258.

[6] Moake, J.L., Turner, N.A., Statopoulos, N.A., Nolasco, L., & Hellums, J.D., Shear-induced Platelet Aggregation can be Mediated by vWf Released from Platelets, as well as by Exogenous Large or Unusually Large vWf Multimers, Requires Adenosine Diphosphate and is Resistant to Aspirin, *Blood*, **71**, 1998, 1366–1374.

[7] Niu, J., Qiao, A.K., and Jiao, L.Q., Hemodynamic Analysis of Stent Expansion Ratio for the Vertebral Artery Ostium Stenosis Intervention, *J. Mech. Med. Biol.*, **13**, 2013, 1350058.

[8] Papafaklis, M.I., Bourantas, C.V., Theodorakis, P.E., Katsouras, C.S., Naka, K.K., Fotiadis, D.I., Michalis, L.K., The Effect of Shear Stress on Neointimal Response Following Sirolimus- and Paclitaxel-eluting Stent Implantation Compared with Bare Metal Stent Sinhumans, *J. Am. Coll. Cardiol. Cardiovasc. Interv.*, **3**, 2010, 1181–1189.

[9] Samady, H., Eshtehardi, P., McDaniel, M.C., Suo, J., Dhawan, S.S., Marynard, C., Timmins, L.H., Quyyumi, A.A., Giddens, D.P., Coronary Artery Wall Shear Stress is Associated with Progression and Transformation of Atherosclerotic Plaque and Arterial Remodeling in Patients with Coronary Artery Disease/Clinical Perspective. *Circulation*, **124**, 2011, 779–788.

[10] Seo, T., Schachter, L.G., Barakat, A.I., Computational Study of Fluid Mechanical Disturbance Induced by Endovascular Stents, *Ann Biomed Eng.*, **33**, 2005, 444–456.

[11] Spijker, H.T., Geaaff, R., Boonstra, R.W., Busscher, H.J., & Van Oeveren, W., On the Influence of Flow Conditions and Wettability on Blood Material Interactions, *Biomaterials*, **24**, 2003, 4717–4727

[12] Stayman, A.N., Nogueira, R.G., Gupta, R., A Systematic Review of Stenting and Angioplasty of Symptomatic Extracranial Vertebral Artery Stenosis, *Stroke*, **42**, 2010, 2212–2216.

[13] Van Belle, E., Tio, F.O., Couffinhal, T., Maillard, L., Pesseri, J., & Isner, J.M., Stent Endothelialization: Time Course, Impact of Local Catheter Delivery, Feasibility of Recombinant Protein Administration, and Response to Cytokine Expedition, *Circulation*, **95**, 1997, 438–448.

[14] Wehman, J.C., Hanel, R.A., Guidot, C.A., Guterman, L. R., Hopkins, N.L., Atherosclerotic Occlusive Extracranial Vertebral Artery Disease: Indications for Intervention, Endovascular Techniques, Short-term and Long-term Results, *J Intervention Cardiol.*, **17**, 2004, 219–232.